Environ. Sci. Technol. **2006**, *40,* 3279−3284

Sorption of PAHs by Aspen Wood Fibers as Affected by Chemical Alterations

LIYUAN HUANG,[†]
THOMAS B. BOVING,[‡] AND
BAOSHAN XING*,[†]

Department of Plant, Soil and Insect Sciences, University of Massachusetts, Amherst, Massachusetts 01003, and Department of Geosciences, University of Rhode Island, Kingston, Rhode Island 02881

Sorption and desorption experiments for phenanthrene and pyrene, using untreated (UTR) and treated (bleaching and hydrolysis) aspen wood fibers, were examined to understand their sorption mechanisms. The wood was characterized by elemental and porosity analysis, solid-state ^{13}C NMR, and diffuse reflectance infrared Fourier transform spectroscopy. Bleaching removed aromatic components, yielding the highest polarity and increased porosity, whereas hydrolysis removed a large percentage of hemicellulose and parts of amorphous cellulose, producing a matrix with more aromatic moieties, lower polarity, and higher porosity than that of the UTR wood fibers. All isotherms fitted well to the Freundlich equation and the *N* values had a decreasing trend from bleached (BL), UTR, low-temperature hydrolyzed to high-temperature hydrolyzed (HHY) wood fibers. BL fibers had the lowest sorption capacity (K_{OC}) for both phenanthrene and pyrene. HHY had the highest K_{OC} because of its high aromatic carbon content and low polarity. The results suggest that aromatic moieties and polarity of wood fibers play significant roles in polycyclic aromatic hydrocarbon (PAHs) sorption and desorption. Thus, both aromatic components and polarity should be considered when predicting the PAHs sorption/desorption by aspen wood fibers. This study demonstrated that aspen wood fibers are a potential sorbent for PAHs and that chemical modifications of the wood matrix can effectively increase its sorption efficiency. These results may have implications for the treatment of stormwater runoff and other PAH-contaminated liquids.

Introduction

Persistent organic pollutants, such as polycyclic aromatic hydrocarbons (PAHs), are commonly detected at elevated concentrations in stormwater runoff and wastewater streams. PAHs originate from predominantly anthropogenic sources, such as incomplete combustion of fuels and discharges from industrial and wastewater treatment plants. Once in the environment, PAHs are recalcitrant due to their low solubility and resistance to biodegradation. Some PAHs are carcinogenic and exhibit toxicity even at a very low concentration (*1*, *2*). A number of conventional and innovative treatment methods for PAH-contaminated water have been developed. Although activated carbon is probably one of the most effective conventional methods for the removal of PAHs from water, its comparably high cost typically prohibits the treatment of large amounts of wastewater and stormwater streams. Thus, innovative filter materials have been proposed that rely on low cost and readily available natural materials (*3*). A few studies (*4*−*6*) examined the sorption of organic chemicals to wood and wood products. All these studies observed linear isotherms of nonpolar compounds for water-saturated woods. However, Gunasekara and Xing (*7*) observed nonlinear isotherms for naphthalene by lignin, a major component of wood. Wood is a heterogeneous material and consists of three major components, cellulose, hemicellulose, and lignin. The chemical differences among these three components result in significant variability in the wood's ability to interact with water and organic contaminants. For instance, cellulose and hemicellulose provide for strong hydrogen bonding as a result of their polyhydroxyl and polycarboxylic structures. Conversely, the lignin phenylpropane units may provide for relatively hydrophobic regions, therefore, attracting hydrophobic compounds. Mackay and Gschwend (*4*) observed that wood−water partition coefficients for monoaromatic hydrocarbons exhibited a positive relationship with the wood's fractional lignin content, probably because cellulose and hemicelluloses contributed very little to the uptake of those chemicals (*8*). A similar result was reported by Garbarini and Lion (*9*) when they studied the sorption of toluene and trichloroethylene to wood polymers. In studying sorption of 2,4-dichlorophenol and 2,4,5-trichlorophenol by pulped wood fibers, Severtson and Banerjee (*6*) demonstrated that sorption is governed by the interaction of the acid form of these compounds with lignin, and, quite interestingly, their results also showed that sorption was unaffected by fiber surface area. Although these past studies were very elegant in their execution and provided useful data, exact sorption mechanisms by the wood and methods to improve its sorption capacity remain largely unknown. Further, structural characteristics of wood samples and their relationship with its sorption capacity and nonlinearity have yet to be studied in detail. Advances in these areas of research could provide new directions for the application of wood-based wastewater filters. The objectives of this study were to characterize in detail untreated (UTR) and chemically modified aspen wood (*Populus tremula*) fibers by using elemental and porosity analysis, solid-state ^{13}C NMR, and diffuse reflectance infrared Fourier transform spectroscopy (DRIFTS). Batch experiments were employed to examine the sorption/desorption behaviors of two common PAHs (pyrene, phenanthrene) with aspen wood fibers and determine the relationship of PAHs sorption/desorption with the porosity, polarity, and structural components (e.g., aromatic moieties). Aspen wood was selected as the study material because it is readily available in fiber form and has already been proven to effectively remove PAHs under laboratory conditions (*5*).

Materials and Methods

Sorbent. UTR aspen wood fibers (length: up to 30 cm, with a diameter of approximately 1 mm) were obtained from the American Excelsior Company, Arlington, TX. Two different chemical treatments were used to remove predetermined structural components from the aspen wood. First, bleaching removed aromatic components (*7*) by treating 10 g of dry aspen wood three times with 100 g of sodium chlorite, 100 mL of acetic acid, and 1000 mL of deionized distilled water

* Corresponding author phone: (413)545-5212; fax: (413)545-3958; e-mail: bx@pssci.umass.edu.
[†] University of Massachusetts.
[‡] University of Rhode Island.

10.1021/es0524651 CCC: $33.50
Published on Web 04/07/2006

for ~7 h for each time. Bleached samples are referred to as BL. The second treatment (hydrolysis) involved treating aspen wood fibers with 300 mL of 6 M HCl/g dry wood. Low-temperature hydrolysis (LHY) was performed at 70 °C for 2 h, followed by hydrolysis at room temperature for another 18 h. High-temperature hydrolysis (HHY) was conducted under refluxing conditions (~100 °C) for 2.5 h. Following the chemical treatments, the solid residue was separated from the solution and rinsed with deionized distilled water. All wood samples were freeze-dried, cut into 2−10 mm long segments, and stored in capped containers.

Characterization of Sorbents. Dry weight-based C, H, and N contents of all samples were determined using a Vario ELIII elemental analyzer (Elementar, Germany) with the oxygen concentration calculated by mass difference. The ash content was measured by heating the wood samples at 740 °C for 4 h. Effective polarity (PI) was calculated by: PI = 0.702 − 0.00353AR, where AR is the percent of aromatic C, as measured using solid-state CPMAS ^{13}C NMR (*8*). The mass atomic ratio, [(N + O)/C] of sorbents, was calculated by their elemental compositions and atomic weights of O, N, and C. Porosity of all samples was determined using a Nova 2000 Brunauer−Emmett−Teller (BET)-N_2 Analyzer (Boynton Beach, FL). Samples were degassed at 90 °C for 10 h prior to the adsorption measurements. The micropore volume was calculated by the Dubinin−Raduskhevich equation at P/P_0 = 0.05 (*10*). The total pore volume (including micropores and mesopores) was determined at P/P_0 = 0.95. Macropore volume was negligibly small, then, mesopore volume was computed as the difference between total and micropore volumes (*11*). Surface area was calculated using the multi-point BET method (*12*). Solid-state CPMAS-TOSS ^{13}C NMR spectra were obtained with a Bruker DSX-300 spectrometer (Karlsruhe, Germany) operated at the ^{13}C frequency of 75 MHz. Except for the number of scans (3000−6000), the instrument was run under the same condition as the one used by Chen et al. (*13*). Within the 0−220 ppm chemical shift range, structural carbon assignments were: aliphatic carbons (0−50 ppm), methoxyl carbons (50−61 ppm), carbohydrate carbons (61−96 ppm), anomeric carbons (96−109 ppm), aromatic carbons (109−165 ppm), carboxyl and carbonyl carbons (163−190 ppm), and ketone carbons (190−220 ppm). All samples were analyzed by DRIFTS using a Perkin-Elmer (Spectrum One) infrared spectrophotometer (Welleslay, MA), following the procedure of Chen et al. (*13*).

Sorption Experiment. ^{14}C-labeled and unlabeled phenanthrene (>98% purity) and pyrene (>99% purity) were purchased from Sigma-Aldrich Chemical company and were used without further purification. For the batch sorption isotherm experiments 8-, 15-, or 35-mL vials were used. The background solution (pH 7) consisted of 0.01 M $CaCl_2$ in deionized distilled water with 200 mg/L NaN_3 as a biocide. As a result of their low water solubility (Table S1, see the Supporting Information), stock labeled and unlabeled phenanthrene and pyrene solutions were prepared in methanol before adding to the aqueous background solution, and the aqueous solution was mixed for approximately 2 h. Initial concentrations of solutes were controlled to have the final equilibrium concentration ranges about 2.5 orders of magnitude (*12*). The total amount of methanol in the solution did not exceed 0.1% volume. The solute-containing solution was added to the vials with the wood fibers. The solid−solution ratios were adjusted to obtain 30−85% sorption of solutes at apparent equilibrium. Each isotherm had 9−12 concentration points; each point, including blanks (i.e., without wood fibers) was run in duplicate. The vials were sealed with aluminum-foil-lined Teflon screw caps and were kept shaking 3 d for phenanthrene and 4 d for pyrene at 23 ± 1 °C. Preliminary experiments indicate that apparent equilibrium was reached before 3 d for phenanthrene and before 4 d for pyrene (Figure S1, see the Supporting Information). After equilibration, the vials were centrifuged at 2800 rpm for 20 min, and approximately 0.8 mL of the supernatant was added to a ScintiVerse cocktail (7 mL) for scintillation counting (Bechman [Fullerton, CA] LS6500). The solute loss was less than 4% of the initial concentrations, which is within the experimental uncertainty range of the analyses by scintillation counting; therefore, sorbed chemical concentrations were determined by mass balance calculations. All sorption data were fitted to the Freundlich equation:

$$S = K_F C^N$$

where S is the sorbed concentration (μg/g), C is the liquid-phase equilibrium solution concentration (μg/mL), K_F is the sorption capacity coefficient [(μg/g)/(μg/mL)^N], and N (dimensionless) is the Freundlich exponent that describes isotherm nonlinearity.

Desorption Experiment. Immediately after completion of the sorption experiments, desorption experiments were performed by sequential decant−refill steps (*14*). Five concentrations were used for the desorption experiment. Solids were separated from the aqueous solutions by centrifugation at 2800 rpm for 20 min. About half of the supernatant (including ~0.8 mL for liquid scintillation counting) was exchanged with the same amount of background solution. The sealed vials were shaken 3 d for phenanthrene and 4 d for pyrene at 23 ± 1 °C. The suspensions were centrifuged and around 0.8 mL of supernatant was analyzed. The above desorption experiment was repeated two more times. After each desorption step, the concentration of labeled phenanthrene or pyrene was determined by liquid scintillation counting. The amount of sorbate remaining on the wood at each desorption step was calculated as the difference between the initially sorbed and the initially desorbed amount. The total desorption percentage was calculated by the sum of three consecutive desorbed amounts (μg/g) divided by the initial sorbed concentration (μg/g).

Results and Discussion

Elemental Composition. The elemental compositions of the four wood samples are shown in Table 1. The ash content of each sample was less than 0.3% of the total weight. BL had the lowest C content and highest O content, thus, the highest polarity. In contrast, HHY had the highest C content but lowest O content, thus, the lowest polarity. LHY had a similar [(N + O)/C] but its PI was lower than UTR. This shows that the chemical treatments successfully changed the chemical composition of the wood matrix.

Porosity Analysis. Except the slight decrease of BL's micropore volume, both bleaching and hydrolysis greatly enhanced the total porosity (Table 1). For instance, the micropore volume was three and eight times greater for LHY and HHY, respectively, compared to that of UTR. The mesopore volume was about 3 (BL), 5 (LHY), and 39 (HHY) times higher, and the surface area was about 3 (BL), 8 (LHY), and 15 (HHY) times larger compared to those of UTR.

Solid-State ^{13}C NMR. ^{13}C NMR results of four samples are presented in Figure 1 and Table S2. The peaks around 21 and 172 ppm were assigned to the methyl C and carbonyl C in acetyl groups of hemicellulose, respectively (*15*). The 55.8 ppm peak was from methoxy groups (OCH_3), which are probably the most characteristic functional group for lignin. The signals located at 83 and 88 ppm were from C-4 in amorphous and crystalline celluloses, respectively. The peaks between 71 and 74 ppm were assigned to C-2, C-3, and C-5 in cellulose, whereas the strong peak at 104 ppm was associated with anomeric carbon (C-1). The peaks in the region of 131−137 ppm were assigned to the ring carbons

TABLE 1. Elemental Composition, Polarity, and Porosity of Four Aspen Wood Samples

sample[a]	C (%)	O[b] (%)	H (%)	N (%)	(N + O)/C	AR[c]	PI[d]	V_{micro}[e] (cm^3/g)	V_{meso}[f] (cm^3/g)	V_T[g] (cm^3/g)	SA[h] (m^2/g)
UTR	46.7	46.6	6.38	0.340	0.754	14.2	0.670	0.0006	0.0006	0.0012	0.62
BL	43.4	50.2	6.26	0.126	0.870	7.50	0.693	0.0005	0.0017	0.0022	2.11
LHY	46.7	46.6	6.52	0.164	0.752	17.9	0.657	0.0016	0.0032	0.0049	4.74
HHY	57.6	36.9	5.49	0.055	0.481	32.7	0.605	0.0049	0.0233	0.0282	9.39

[a] UTR, untreated aspen wood; BL, bleached aspen wood; LHY and HHY, hydrolyzed aspen wood under low temperature and high temperature (~100 °C), respectively. [b] Oxygen content was calculated by the mass difference. [c] AR = percent aromatic C, as measured by CPMAS ^{13}C NMR. [d] PI (effective polarity) = 0.702 − 0.00353AR. [e] V_{micro}: micropore volume calculated from the equation of Dubinin−Raduskhevich. [f] V_{meso}: mesopore volume calculated by the difference between total pore volume and micropore volume. [g] V_T: total pore volume measured as the amount of nitrogen adsorbed at $P/P_0 = 0.95$ (*11*). [h] SA: surface area calculated from the multi-point BET method (*12*).

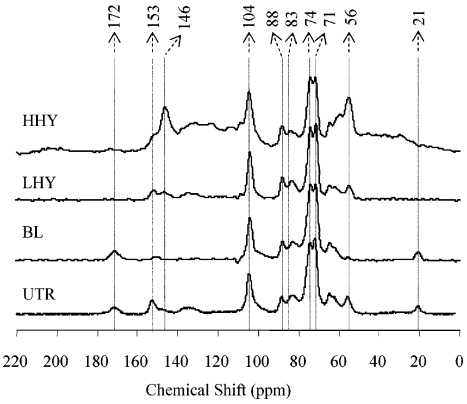

FIGURE 1. Solid-state ^{13}C NMR spectra of UTR, BL, LHY, and HHY. Aliphatic C (0−109 ppm), aromatic C (109−163 ppm), and COOH/C═O (163−220 ppm).

in which the ring was not substituted by strong electron donors such as oxygen and nitrogen (*16*). The multiple peaks in the range from 145 to 163 ppm were from the carbons of phenolic components, mainly the syringyl and guaiacyl units in lignin (*17*). The peak around 153 ppm was due to C-3 and C-5 of the syringyl units involved in ether linkages at C-4 and C-3 and C-4 in the guaiacyl units (*18*). The peak at 146 ppm was from C-4 in the guaiacyl unit with free phenolic OH at C-4 (*17*).

The ^{13}C NMR spectra illustrate that bleaching and hydrolysis caused structural modifications of aspen wood matrix. Most notably, bleaching reduced the fraction of the aromatic carbon (109−163 ppm) from 14.2 to 7.5%. The removal of aromatic components increased the PI from 0.670 to 0.693 (Table 1). Hydrolysis effectively removed hemicelluloses in both hydrolyzed samples, which is supported by the almost disappearance of the peaks around 21 and 172 ppm in LHY and HHY. Consequently, the aromatic C increased to 17.9% for LHY and 32.7% for HHY. Further, the increase of the peak at 88 ppm in LHY and HHY indicates that hydrolysis enhanced the crystallinity of cellulose. Hence, hydrolysis led to a more hydrophobic material because O-containing moiety content was reduced and sorption of water by crystalline cellulose is less than amorphous cellulose (*19*).

Concurrent with the increasing signals of aromatic C in the region of 109−163 ppm in HHY, the intensity of the 55.8 ppm peak increased significantly. Also, the increasing intensities at 146 ppm indicate the cleavage of aryl ether in wood lignin by the formation of the phenolic hydroxyl group (*20*). Moreover, the intensities around 131−137 ppm in HHY were much stronger than that of other samples. The shift of maximum peaks reveals an alteration of hydrolyzed aspen wood that concurred with changes of the porosity and polarity of the wood matrix. Similar evidence was presented by Pisarnitsky et al. (*21*), who found that heating of oak wood under acid conditions changed the aromatic characteristic of the oak because of increasing its relative content of guaiacol, syringyl, acetovanillon, and propiovanillon.

DRIFTS. The DRIFT spectra between 4000 and 450 cm^{-1} for the four wood samples are presented in Figure 2. A broad and strong band in the region from 3324 to 3346 cm^{-1} was assigned to the stretching vibration of the hydroxyl group, indicative of hydrogen bonding. The absence of absorption around 3600 cm^{-1} suggests that there were no appreciable free hydroxyl groups present in these four samples (*13*). A strong methylene/methyl vibration was observed at 2895 cm^{-1} in UTR, BL, and LHY (2939 cm^{-1} for HHY).

The absorption bands at 1740 cm^{-1} mainly arose from the carbonyl (C═O) linkage in acetyl ester groups from hemicellulose (*22*). Because carbonyl groups occur abundantly within the polymer components of wood, they tend to dominate in the branched-chain hemicellulose polymer (*23*). It is evident that ester carbonyl groups from hemicellulose dominated in UTR and BL. However, this DRIFT band became obscure in the two hydrolyzed samples because hemicellulose was readily decomposed under acid conditions (*24*). Conversely, the absorption bands around 1718 (LHY) and 1704 cm^{-1} (HHY) were attributed to the carbonyl stretching of unconjugated ketone and conjugated carboxylic groups in lignin (*25*). This indicates that the C═O group is only weakly H-bonded (*26*). The intensity of the carbonyl group was remarkably lower in LHY than in the other samples. Conversely, it was high in HHY, showing that some ether linkages in lignin or lignincellulose complexes, such as β-O-4 linkages, were cleaved under high temperature (*27*).

The absorption bands at 1595 and 1505 cm^{-1} were assigned to aromatic ring carbon skeletal stretching (*22*, *24*). The 1595 cm^{-1} band was also attributive to the stretching of the conjugated C═O group (*28*). These two bands were similar in UTR and LHY, but almost completely disappeared in BL. In contrast, and consistent with the NMR data, these bands became very strong in the HHY. This indicates for one that bleaching caused the cleavage of the aromatic ring and, second, hydrolysis under high temperature led to the increase of aromatic moieties.

Absorption bands around 1462 and 897 cm^{-1} were ascribed to CH and CH_2 units. The band at 1462 cm^{-1} was assigned to C−H deformation in methyl and methylene in the syringyl unit from lignin (*29*). It became sharper and stronger after hydrolysis at high temperature, but weaker after bleaching. The band at 897 cm^{-1} was assigned to CH_2 wagging from carbohydrates (*28*, *29*). Its relative intensity was strong in UTR, BL, and LHY, but almost disappeared in HHY.

Absorption bands at 1273, 990, and 617 cm^{-1} were from C−O single bonded in carbohydrates (*23*). Generally, the intensities of these bands were decreasing in the following order: BL, UTR, LHY, and HHY. This underlined that hemicellulose and parts of cellulose were easy to hydrolyze in an acidic environment, especially at high temperature. However, the absorption band at 1250 cm^{-1} was attributable to C−O single bonds in lignin (*28*). A pronounced intensity

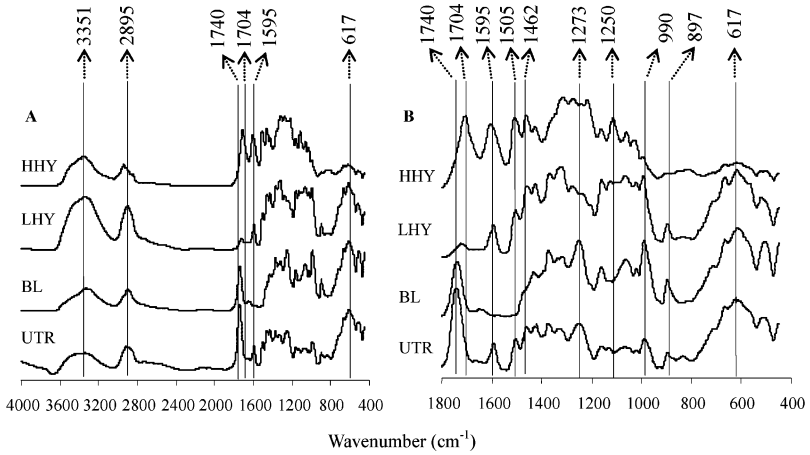

FIGURE 2. DRIFT spectra of UTR, BL, LHY, and HHY. A, 450−4000 cm^{-1}; B, 450−1800 cm^{-1}.

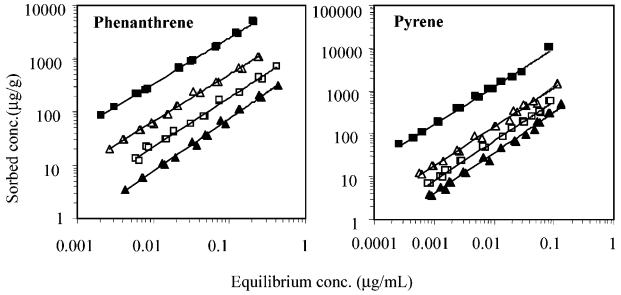

FIGURE 3. Sorption isotherms of phenanthrene and pyrene by UTR (□), BL (▲), LHY (△), and HHY (■). The *y*-axis scale is different for phenanthrene and pyrene.

increase of this peak was observed in HHY. These data again suggest that the relative lignin content was higher after hydrolysis but lower after bleaching. This finding is in good agreement with the NMR results.

Sorption of Phenanthrene and Pyrene. Sorption isotherms were fitted well to the Freundlich model (Figures 3 and S2). The Freundlich exponent, *N* (Table 2) ranged from 0.869 to 0.985 for phenanthrene and from 0.900 to 0.948 for pyrene. Except for that of BL, all isotherms were nonlinear. Nonlinearity was also reported by Mackay (*30*) and likely resulted from aromatic moieties that are responsible for condensed domains (*7*). Xing (*31*) observed that there was a positive relationship between aromatic carbons and isotherm nonlinearity for several soil humic acids. For both phenanthrene and pyrene, removal of large percentages of aromatic moieties by bleaching apparently resulted in a more linear, partition-type sorption, while the increase in aromaticity after hydrolysis led to more nonlinear, adsorption-type behavior; however, some isotherm *N* values were not significantly different (Table 2). Nonlinear isotherms in this work differed from the results of some previous studies (*4*−*6*) in which linear isotherms were observed for wood materials. Mackay and Gschwend (*4*) explained that nonlinear isotherms of benzene to pine sawdust (*30*) may be due to the incomplete water saturation of the wood. However, 3 days were sufficient to achieve water saturation of thin aspen wood fibers in our experiments. It appears that linear sorption in the aforementioned studies may also be due to relatively high solute concentrations and/or narrow concentration ranges.

A precise comparison between K_F values is not possible due to their different units as a result of nonlinearity (*32*). Hence, concentration-dependent organic carbon-normalized sorption capacity (K_{OC}) was calculated by the content of the organic carbon of wood sample and K_d values at three equilibrium concentrations (Table 2). Bleaching and hydrolysis resulted in great differences in K_{OC}. For instance, BL's K_{OC} values were only about 40% for phenanthrene and 60% for pyrene relative to those of UTR. However, K_{OC} values of LHY were about two (pyrene) and three (phenanthrene) times greater than those of UTR. Even greater K_{OC} values were determined for HHY (i.e., eleven times larger for phenanthrene and fourteen times higher for pyrene relative to UTR). A positive relationship between K_{OC} values and aromatic C content was observed (Figure 4A). This may be attributed to hydrophobic effect, $\pi-\pi$ electron donor−acceptor ($\pi-\pi$ EDA) interactions, and polarizability effect (*33*−*35*). Aromatic rings in lignin-type structures may favor polarizable interactions with organic solutes, especially those with high polarizability such as pyrene and phenanthrene. Zhu et al. (*33*, *34*) reported the importance of $\pi-\pi$ EDA interactions between π-donors such as PAHs and π-acceptor groups in natural organic matter including polycarboxylated aromatic rings. In studying the effect of the quality of soil

TABLE 2. Sorption Coefficients and Freundlich Model Parameters of Phenanthrene and Pyrene by Aspen Wood Samples

					K_{OC} (μg/g OC)		
					equilibrium concentration (μg/mL)		
PAH	sample	log K_F [c]	*N*	R^2	*C* = 0.01	*C* = 0.05	*C* = 0.1
PHEN[a]	UTR	3.19 ± 0.028	0.928 ± 0.019	0.997	4660	4150	3940
	BL	2.83 ± 0.019	0.985 ± 0.013	0.996	1800	1750	1740
	LHY	3.59 ± 0.023	0.887 ± 0.013	0.996	14 000	11 700	10 800
	HHY	4.26 ± 0.014	0.869 ± 0.007	0.999	57 500	46 600	42 600
PY[b]	UTR	3.67 ± 0.028	0.922 ± 0.013	0.995	14 400	12 700	12 000
	BL	3.45 ± 0.047	0.948 ± 0.022	0.994	8200	7600	7300
	LHY	3.99 ± 0.044	0.912 ± 0.019	0.994	31 075	27 000	25 400
	HHY	4.89±0.044	0.900 ± 0.019	0.994	214 000	182 000	170 000

[a] PHEN: phenanthrene. [b]PY: pyrene. [c] K_F unit = (μg/g)(μg/mL)$^{-N}$

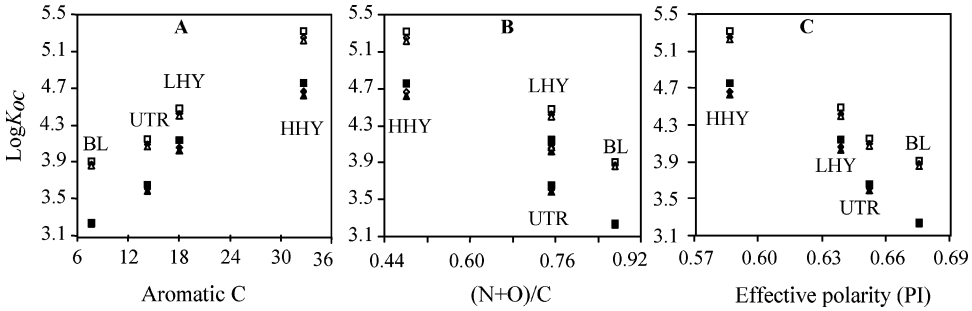

FIGURE 4. Relationship between log K_{OC} and aromatic carbon content (A), mass ratio [(N + O)/C] (B), or PI (C) at three equilibrium concentrations: phenanthrene, 0.01 (■), 0.05 (◆), and 0.1 μg/mL (▲); pyrene, 0.01 (□), 0.05 (◇), and 0.1 μg/mL (△).

organic matter on sorption of naphthalene, Xing (*36*) reported that the K_{OC} values increased with increasing aromaticity. Similar results were reported by Young and Weber (*37*). Furthermore, several studies (*8*, *9*) indicated that cellulose and hemicelluloses, which mainly consist of polar aliphatic moieties, exhibit little measurable uptake of monoaromatic hydrocarbons, while lignin, containing primarily aromatic moieties, showed great affinity for hydrocarbons. This is confirmed by the results from Kleinert (*38*), who found that isolated lignin took up 3.53 mmol phenol/g, whereas only 0.025 mmol phenol/g were sorbed to isolated amorphous cellulose.

In addition to aromatic moieties, the polarity of the sorbent can significantly affect the sorption capacity of organic contaminants (*13*, *39*). In this study, the polarity, (N + O)/C, of the four samples was in the following order: BL > UTR ~ LHY > HHY. Figure 4B shows an apparently negative relationship between the K_{OC} values and (N + O)/C of the sorbents. HHY with the lowest polarity had the greatest K_{OC} values, followed by LHY, UTR, and BL. In studying cross-correlation of polarity curves to predict sorption coefficients of nonionic organic contaminants, Xing et al. (*8*) used the PI to more accurately predict the K_{OC} for soil organic matter. This is because polarity expressed by [(O + N)/C] does not consider the effect of configuration and structure on sorption. As shown in Figure 4C, when PI is used (*8*), a clear relationship is obtained over that between K_{OC} and [(O + N)/C], indicating that the location of O and N in the chemical structure of the wood can be important for sorption. For UTR, lignin-rich moieties may be dispersed among carbohydrates rich in polyhydroxyl and carboxylic groups (*30*). These functional groups can produce strong hydrogen bonds within the wood and also with water. This may prevent PAH molecules from accessing the aromatic cores as a result of the surrounding polar components (*13*). For LHY, however, hydrolysis destroyed some of those hydrogen bonds and modified the structure and configuration of the wood, leading to the decrease of PI from 0.670 to 0.657. Thus, PAH molecules might more easily get access to the aromatic cores of the hydrolyzed wood, which increased the K_{OC} in comparison with that of UTR.

In this study, HHY had the greatest K_{OC} values and the highest porosity, followed by LHY, BL, and UTR in terms of porosity. HHY showed much higher porosity than that of other samples, which may partly contribute to its high sorption capacity. However, the BL matrix had a higher porosity than that of UTR but its K_{OC} values were lower. Thus, the porosity might not be the primary factor regulating sorption capacity.

PAH Desorption. Desorption data are presented in Figure S3 and S4 (see the Supporting Information). Differences in the degree of hysteresis were observed between chemically treated samples. For instance, in BL, no desorption hysteresis took place at all phenanthrene and pyrene concentrations. Conversely, for HHY, pronounced hysteresis occurred at all concentrations of phenanthrene and pyrene, reflecting that desorption of these compounds from this wood matrix was comparatively difficult. The possible reasons for the difference in hysteresis between these wood samples may be as follows. First, bleaching successfully removed a large part of the aromatic moieties and produced a more expanded matrix (consisting of mainly holocellulose) in which a reversible sorption mechanism dominated. In contrast, hydrolysis, especially under high temperature, removed most hemicellulose and part of the cellulose, yielding a much more condensed matrix in which irreversible adsorption might dominate. In studying the sorption of phenol, Kleinert (*38*) found that adsorption by cellulose followed the Henry's reversible solution equilibrium law, while sorption by isolated lignin was described well by the Freundlich equation. These results reveal that aromatic moieties also play an important role in hysteresis, that is, the higher aromaticity, the more apparent hysteresis. Second, desorption behavior was also affected by polarity. For BL, high polarity may have weakened the interactions between this sorbent and PAH molecules (*40*), which contributed to the easy release of PAH molecules from the wood matrix. On the contrary, PAH molecules were slightly desorbed from the low-polarity samples, LHY and HHY, because of strong hydrophobic interactions and $\pi-\pi$ EDA interactions (*34*). Additionally, higher porosity of HHY may have resulted in more retarded desorption in comparison with that of other samples.

In conclusion, our results demonstrate that both aromatic moieties and polarity are important for PAH sorption and desorption in aspen wood fibers. The K_{OC} values increased with increasing aromatic moieties and with decreasing polarity of the sorbent. This study also indicates that PI can predict the sorption capacity of aspen wood fibers more accurately than mass atomic ratio, [(N + O)/C], because PI considers sorbent configuration and structure. Furthermore, structural modifications could substantially enhance the K_{OC} and retention time of PAHs, which is critical for developing novel and low-cost technologies for the remediation of wastewater using wood materials.

Acknowledgments

This work was supported by the McIntire-Stennis program (MAS 00090) and the Federal hatch program (MAS 8532). We acknowledge the American Excelsior Company (Mr. Tony Johnson) for providing us with wood samples.

Supporting Information Available

Chemical and physical properties of phenanthrene and pyrene (Table S1), phenanthrene sorption and desorption kinetics of UTR and HHY (Figure S1), structural carbon distributions as obtained from ^{13}C NMR (Table S2), comparisons of linear and nonlinear isotherms of phenanthrene and pyrene for UTR, BL, LHY, and HHY (Figure S2), desorbed percentages of phenanthrene and pyrene from four samples (Figure S3), and sorption and desorption isotherms of

phenanthrene and pyrene (Figure S4). This material is available free of charge via the Internet at http://pubs.acs.org.

Literature Cited

(1) Monson, P. D.; Ankley, G. T.; Kosian, P. A. Phototoxic response of iumbriculus-variegatus to sediments contaminated by polycyclic aromatic-hydrocarbons. *Environ. Toxicol. Chem.* **1995**, *14*, 891−894.

(2) Arfsten, D. P.; Schaeffer, D. J.; Mulveny, D. C. The effects of near-ultraviolet radiation on the toxic effects of polycyclic aromatic hydrocarbons in animals and plants: A review. *Ecotoxicol. Environ. Safe* **1996**, *33*, 1−24.

(3) Low, K. S.; Lee, C. K.; Mak, S. M. Sorption of copper and lead by citric acid modified wood. *Wood Sci. Technol.* **2004**, *38*, 629−640.

(4) Mackay, A. A.; Gschwend, P. M. Sorption of monoaromatic hydrocarbons to wood. *Environ. Sci. Technol.* **2000**, *34*, 839−845.

(5) Boving, T. B.; Zhang, W. Removal of aqueous-phase polynuclear aromatic hydrocarbons using aspen wood fibers. *Chemosphere* **2004**, *54*, 831−839.

(6) Severtson, S. J.; Banerjee, S. Sorption of chlorophenols to wood pulp. *Environ. Sci. Technol.* **1996**, *30*, 1961−1969.

(7) Gunasekara, A. S.; Simpson, M. J.; Xing, B. S. Identification and characterization of sorption domains in soil organic matter using structurally modified humic acids. *Environ. Sci. Technol.* **2003**, *37*, 852−858.

(8) Xing, B. S.; McGill, W. B.; Dudas, M. J. Cross-correlation of polarity curves to predict partition-coefficients of nonionic organic contaminants. *Environ. Sci. Technol.* **1994**, *28*, 1929−1933.

(9) Garbarini, D. R.; Lion, L. W. Influence of the nature of soil organics on the sorption of toluene and trichloroethylene. *Environ. Sci. Technol.* **1986**, *20*, 1263−1269.

(10) Ismail, I. M. K.; Rodgers, S. L. Comparisons between fullerene and forms of well-known carbons. *Carbon* **1992**, *30*, 229−239.

(11) Sanchez, A. R.; Elguezabal, A. A.; Saenz, L. D. CO_2 activation of char from Quercus agrifolia wood waste. *Carbon* **2001**, *39*, 1367−1377.

(12) Yang, K.; Zhu, L. Z.; Xing, B. S. Adsorption of polycyclic aromatic hydrocarbons by carbon nanomaterials *Environ. Sci. Technol.* **2006**, *40*, 1855−1861.

(13) Chen, B. L.; Johnson, E. J.; Chefetz, B.; Zhu, L. Z.; Xing, B. S. Sorption of polar and nonpolar aromatic organic contaminants by plant cuticular materials: Role of polarity and accessibility. *Environ. Sci. Technol.* **2005**, *39*, 6138−6146.

(14) Weber, W. J.; Kim, S. H.; Johnson, M. D. Distributed reactivity model for sorption by soils and sediments. 15. High-concentration co-contaminant effects on phenanthrene sorption and desorption. *Environ. Sci. Technol.* **2002**, *36*, 3625−3634.

(15) Martinez, A. T.; Gonzalez, A. E.; Prieto, A.; Gonzalezvila, F. J.; Frund, R. Para-hydroxyphenyl-guaiacyl-syringyl ratio of lignin in some austral hardwoods estimated by CuO-oxidation and solid-state NMR. *Holzforschung* **1991**, *45*, 279−284.

(16) Schnitzer, M.; Preston, C. M. Effects of acid-hydrolysis on the C-13 NMR-spectra of humic substances. *Plant Soil* **1983**, *75*, 201−211.

(17) Hawkes, G. E.; Smith, C. Z.; Utley, J. H. P.; Vargas, R. R.; Viertler, H. A comparison of solution and solid-state C-13 NMR-spectra of lignins and lignin model compounds. *Holzforschung* **1993**, *47*, 302−312.

(18) Haw, J. F.; Maciel, G. E.; Biermann, C. J. C-13 nuclear magnetic-resonance study of the rapid steam hydrolysis of red oak. *Holzforschung* **1984**, *38*, 327−331.

(19) Pizzi, A. The water sorption isotherm of crystalline cellulose I and II and amorphous cellulose. A molecular mechanics approach. *Cellul.: Chem., Biochem. Mater. Aspects* **1993**, 217−224.

(20) Lai, Y. Z.; Guo, X. P. Acid-catalyzed hydrolysis of aryl ether linkages in wood 0.1. Estimation of noncyclic alpha-aryl ether units. *Holzforschung* **1992**, *46*, 311−314.

(21) Pisarnitsky, A. F.; Klimov, S. A.; Brazhnikova, E. V. Effect of acid hydrolysis of oak wood on its aroma-forming complex. *Appl. Biochem. Microbiol.* **2004**, *40*, 613−616.

(22) Ajuong, E. M. A.; Redington, M. Fourier transform infrared analyses of bog and modern oak wood (quercus petraea) extractives. *Wood Sci. Technol.* **2004**, *38*, 181−190.

(23) Kimura, F.; Kimura, T.; Gray, D. G. FT-IR study of UV-irradiated stoneground wood pulp. *Holzforschung* **1992**, *46*, 529−532.

(24) Yang, C.; Huang, W. L.; Xiao, B. H.; Yu, Z. Q.; Peng, P.; Fu, J. M.; Sheng, G. Y. Intercorrelations among degree of geochemical alterations, physicochemical properties, and organic sorption equilibria of kerogen. *Environ. Sci. Technol.* **2004**, *38*, 4396−4408.

(25) Matuana, L. M.; Balatinecz, J. J.; Sodhi, R. N. S.; Park, C. B. Surface characterization of esterified cellulosic fibers by XPS and FTIR spectroscopy. *Wood Sci. Technol.* **2001**, *35*, 191−201.

(26) Cao, Y.; Varo, G.; Klinger, A. L.; Czajkowsky, D. M.; Braiman, M. S.; Needleman, R.; Lanyi, J. K. Proton-transfer from asp-96 to the bacteriorhodopsin schiff-base is caused by a decrease of the p*K*(a) of asp-96 which follows a protein backbone conformational change. *Biochemistry* **1993**, *32*, 1981−1990.

(27) Barker, B.; Owen, N. L. Identifying softwoods and hardwoods by infrared spectroscopy. *J. Chem. Educ.* **1999**, *76*, 1706−1709.

(28) Pandey, K. K. A study of chemical structure of soft and hardwood and wood polymers by FTIR spectroscopy. *J. Appl. Polym. Sci.* **1999**, *71*, 1969−1975.

(29) Herring, A. M.; McKinnon, J. T.; Gneshin, K. W.; Pavelka, R.; Petrick, D. E.; McCloskey, B. D.; Filley, J. Detection of reactive intermediates from and characterization of biomass char by laser pyrolysis molecular beam mass spectroscopy. *Fuel* **2004**, *83*, 1483−1494.

(30) Mackay, A. A. Groundwater fate of aromatic hydrocarbons at industrial sites: A coal tar site case study, Ph.D. Thesis, Massachusetts Institute of Technology, 1998.

(31) Xing, B. S. Sorption of naphthalene and phenanthrene by soil humic acids. *Environ. Pollut.* **2001**, *111*, 303−309.

(32) Chen, Z.; Xing, B. S.; McGill, W. B. A unified sorption variable for environmental applications of the Freundlich equation. *J. Environ. Qual.* **1999**, *28*, 1422−1428.

(33) Zhu, D. Q.; Hyun, S. H.; Pignatello, J. J.; Lee, L. S. Evidence for pi-pi electron donor-acceptor interactions between pi-donor aromatic compounds and pi-acceptor sites in soil organic matter through pH effects on sorption. *Environ. Sci. Technol.* **2004**, *38*, 4361−4368.

(34) Zhu, D. Q.; Pignatello, J. J. A concentration-dependent multiterm linear free energy relationship for sorption of organic compounds to soils based on the hexadecane dilute-solution reference state. *Environ. Sci. Technol.* **2005**, *39*, 8817−8828.

(35) Nguyen, T. H.; Goss, K. U.; Ball, W. P. Polyparameter linear free energy relationships for estimating the equilibrium partition of organic compounds between water and the natural organic matter in soils and sediments. *Environ. Sci. Technol.* **2005**, *39*, 913−924.

(36) Xing, B. S. The effect of the quality of soil organic matter on sorption of naphthalene. *Chemosphere* **1997**, *35*, 633−642.

(37) Young, T. M.; Weber, W. J. J. A distributed reactivity model for sorption by soils and sediments. 3. Effects of diagenetic processes on sorption energetics. *Environ. Sci. Technol.* **1995**, *29*, 92−97.

(38) Kleinert, T. The behavior of cellulose under pressure heating in alcohol-water mixtures. *Cellul. Chem.* **1940**, *18*, 114.

(39) Rutherford, D. W.; Chiou, C. T.; Kile, D. E. Influence of soil organic-matter composition on the partition of organic-compounds. *Environ. Sci. Technol.* **1992**, *26*, 336−340.

(40) Chefetz, B.; Deshmukh, A. P.; Hatcher, P. G.; Guthrie, E. A. Pyrene sorption by natural organic matter. *Environ. Sci. Technol.* **2000**, *34*, 2925−2930.

Received for review December 8, 2005. Revised manuscript received February 27, 2006. Accepted March 13, 2006.

ES0524651